LANGMUIR Article
Cite This: Langmuir 2018, 34, 3806−3812
pubs.acs.org/Langmuir

Ringlike Migration of a Droplet Propelled by an Omnidirectional Thermal Gradient

Qingwen Dai,[†] Wei Huang,[†] Xiaolei Wang,*[,†] and M. M. Khonsari[‡]

[†]College of Mechanical and Electrical Engineering, Nanjing University of Aeronautics & Astronautics, Nanjing 210016, China
[‡]Department of Mechanical and Industrial Engineering, Louisiana State University, 3283 Patrick Taylor Hall, Baton Rouge, Louisiana 70803, United States

Supporting Information

ABSTRACT: The interfacial phenomenon associated with the ringlike motion of a liquid droplet subjected to an omnidirectional thermal gradient is investigated. An experimentally verified model is proposed for estimating the droplet migration velocity. It is shown that the unbalanced interfacial tension acting on the liquid in the radial direction provides the necessary propulsion for the migration, whereas the internal force acting on the adjoining liquid contributes to the equilibrium condition in the circumferential direction. This study puts forward the understanding of the interfacial spreading phenomenon, the knowledge of which is important in applications where liquid lubricants are encountered with directionally unstable thermal gradients.

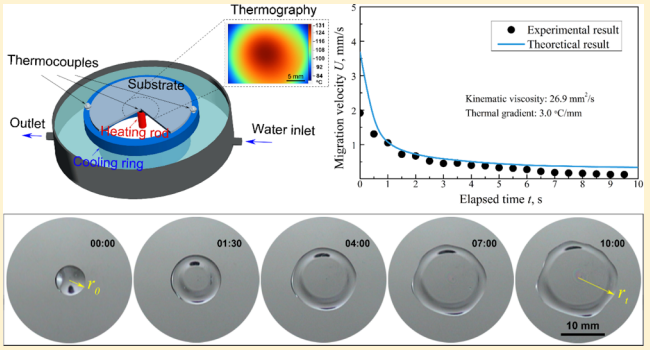

1. INTRODUCTION

Thermocapillary migration of a droplet over a solid substrate is a part of the larger topic known as the Marangoni flows in which the surface tension due to both temperature and chemical composition at the interface provides the driving force. These flows have relevance to a large number of technological applications such as microfluidics, inkjet printing, miniature rolling bearings, and so on.[1−11] Naturally, when dealing with thermocapillary action alone, it is the thermal gradient in the surface tension of a liquid that provides the driving force to induce propelling motion from the high-temperature to low-temperature regions.[12−14] This thermally-driven flow involves the interaction of three phases (solid−liquid−gas) through coupling by heat conduction with the substrate and convection within the droplet.[15−17]

The existing literature contains rich volumes of theoretical research devoted to the interfacial migration phenomenon.[18−27] Among noteworthy and relevant contribution to the subject of this paper is the work of Brochard[28] who developed theoretical models to describe the unidirectional migration of droplets with various cross-section shapes caused by either chemical or thermal gradients. Inspired by that work, Ford and Nadim[29] presented a derivation for droplets with an arbitrary height profile, which takes the slip condition in the vicinity of the contact lines into consideration. Given the fact that the liquid viscosity is significantly affected by temperature, Dai et al.[30] incorporated an appropriate viscosity−temperature relationship into the derivation. These studies provide valuable insights into the unidirectional migration phenomenon induced by the thermal gradient. Nevertheless, they are also suitable for evaluating the unidirectional motion of droplets induced by surface wettability gradient[31,32] or vibration.[33,34]

In treating the unidirectional migration, it is typically assumed that the droplet has a two-dimensional (2-D) arclike shape and that the thin-film lubrication approximation applies or that it takes on the shape of a spherical cap in a three-dimensional model.[35] In applications where the liquid flow is driven by its proximity to a heat source, the temperature distribution on the surface can become heterogeneous and the thermal gradient directionally unstable so that the migration direction becomes uncertain.

Research reveals that under a unidirectional thermal gradient, the droplet of paraffin oil tends to migrate from the high-temperature to low-temperature regions, that is, from left to right as shown in Figure 1a.[30] In the case of an omnidirectional thermal gradient, the flow originates from a single heat source and the temperature decreases uniformity in all directions. Accordingly, the droplet tends to migrate radially outward from the center to the surrounding regions, forming a ringlike motion as shown in Figure 1b.

Examination of the available literature indicates that in contrast to unidirectional migration, there are currently no suitable models available to describe the motion of omnidirectional migration. Hence, we report the results of an experimentally verified model for predicting the ringlike migration of liquid droplets on a solid surface. The theoretical

Received: December 17, 2017
Revised: March 9, 2018
Published: March 12, 2018

DOI: 10.1021/acs.langmuir.7b04259
Langmuir 2018, 34, 3806−3812

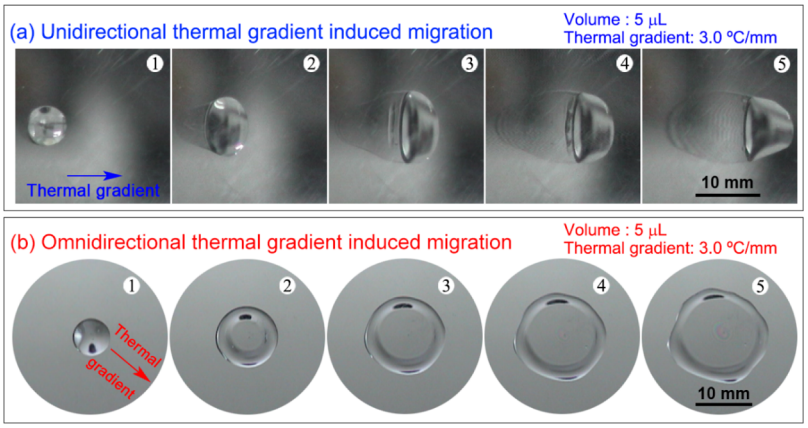

Figure 1. Thermocapillary migration of paraffin oil droplets on the smooth surface induced by a (a) unidirectional thermal gradient[30] and (b) omnidirectional thermal gradient.

model is based on the thin-film lubrication flows and enables one to develop an effective approach for estimating the theoretical migration velocity.

2. THEORETICAL MODEL

It has been proven that the motion of the droplet under a thermal gradient can be recognized as a balance of two forces acting on the droplet:[28] the viscous resistance force (F_v) and the driving force (F_d), which is directly related to the gradients of the solid−liquid interfacial tension. Noting that the existing models for describing forces in unidirectional cases do not apply, we now proceed to derive the governing equations of the forces under an omnidirectional thermal gradient.

Figure 2 shows the geometrical configuration of a migrated droplet with the internal forces within the droplet. A cylindrical

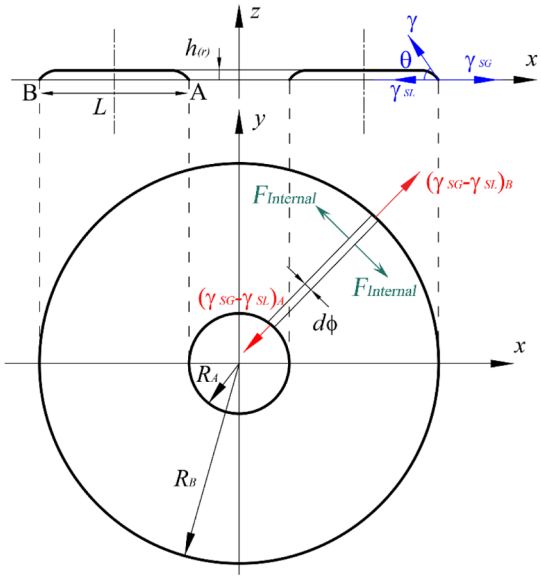

Figure 2. Side and plan views of the footprint of a droplet migrating on a solid surface.

coordinate system (r, ϕ, z) is used to describe the flow in which (r, ϕ) and z represent the horizontal and vertical coordinates, respectively. The following theoretical derivation does not hold for the early stages of spreading, that is, the stages before the ringlike motion is formed because the very small amount of liquid remaining in the middle region is ignored. Our previous research[30] has revealed that at high temperatures, the contact angles of paraffin oil droplets on the stainless steel surface are very small, so the difference of contact angles is ignored in this study.

We assume that the droplet footprint is circular in shape and the height profile of the droplet is denoted by $h(r)$. Because the width (L) and height (h) of the cross section decrease with increasing the radius of ring shape, the cross section of the liquid in one $z-r$ section will always change with time. Nevertheless, for a specified h, one can predict the migration velocity by assuming that the motion at each time interval is quasi-steady. The internal force ($F_{internal}$) acting on the adjoining liquid contributes to the inner balance, whereas the viscous resistance force (F_v) and the driving force (F_d) are deduced as follows.

2.1. Viscous Resistance Force. Applying the thin-film lubrication approximation theory and assuming $V_\phi = 0$, $V_z = 0$, the Navier−Stokes equation reduces to

$$\frac{\partial^2 V_r}{\partial z^2} = \frac{1}{\mu}\frac{\partial P}{\partial r} \tag{1}$$

where V_r is the flow velocity in r direction, P is the pressure field, and μ is the dynamic viscosity, $\mu = \rho\upsilon$ (ρ is the density and υ is the kinematic viscosity).

The reference coordinate system is considered to be traveling with the droplet so that the substrate appears to move toward the center with a velocity U. The boundary conditions at $z = h(r)$ and $z = 0$ are

$$\begin{cases} \dfrac{\partial V_r}{\partial z} = \dfrac{1}{\mu}\dfrac{\partial \gamma}{\partial r}, & z = h(r) \\ V_r = -U, & z = 0 \end{cases} \tag{2}$$

Integrating eq 1, applying the boundary conditions, eq 2, and solving for the velocity field, we have

$$V_r(z) = \frac{1}{\mu}\left[C_T\gamma_T z + \frac{1}{2}\frac{\partial P}{\partial r}(z^2 - 2zh)\right] - U \tag{3}$$

where γ_T is the surface tension coefficient, $\gamma_T = \frac{\partial \gamma}{\partial T}$, and the thermal gradient is assumed to be constant, that is, $\frac{\partial T}{\partial x} = \text{const} = C_T$.

DOI: 10.1021/acs.langmuir.7b04259
Langmuir 2018, 34, 3806−3812

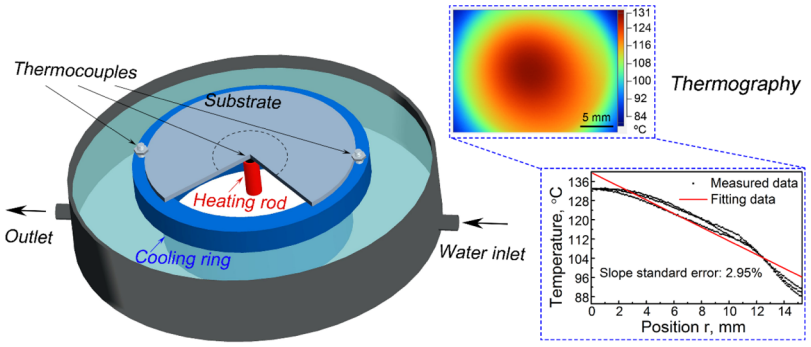

Figure 3. Schematic diagram of the experimental apparatus and the thermography obtained on the substrate surface.

Because no volumetric flux passes through the vertical cross section of the droplet in the z-direction, we can write

$$\int_0^h V_r(x, y, z)\, dz = 0 \tag{4}$$

Then, the pressure gradient satisfying this constraint is given by

$$\frac{\partial P}{\partial r} = -\frac{3\mu}{h^2}U + \frac{3}{2h}C_T\gamma_T \tag{5}$$

The viscous stress σ_{zr} at the liquid−solid interface ($z = 0$) is

$$\sigma_{zr(z=0)} = \mu\left(\frac{\partial u_r}{\partial z}\bigg|_{z=0}\right) = \frac{3\mu}{h}U - \frac{1}{2}\gamma_T C_T \tag{6}$$

The hydrodynamic force (F_v) exerted by the solid surface is obtained by integrating the viscous stress

$$F_v = \iint_A \{\sigma_{rz}\}_{(z=0)}\, dA = \int_0^{2\pi}\int_{R_A}^{R_B} \sigma_{rz} r\, dr\, d\phi$$
$$= \frac{6\pi\mu(R_B)}{h}U - \frac{\pi}{2}\gamma_T C_T(R_B{}^2 - R_A{}^2) \tag{7}$$

2.2. Driving Force. The Young's equation defines the interfacial tension force balance and contact angle in the vicinity of the three-phase contact line[36]

$$\gamma_{SG} = \gamma_{SL} + \gamma\cos\theta \tag{8}$$

where θ is the equilibrium contact angle.

The unbalanced interfacial tension forces subjected to an omnidirectional thermal gradient constituting the driving force (f_d) for per unit length is

$$f_d = (\gamma_{SG} - \gamma_{SL})_B - (\gamma_{SG} - \gamma_{SL})_A \tag{9}$$

Combining eqs 8 and 9, we arrive at the following expression for the driving force per unit length

$$f_d = \gamma_T C_T(R_B - R_A)\cos\theta \tag{10}$$

Then, the driving force (F_d) exerted on the droplet is

$$F_d = \int_0^{2\pi} f_d(R_B - R_A)\, d\phi$$
$$= 2\pi\cos\theta(R_B - R_A)^2\gamma_T C_T \tag{11}$$

Note that the liquid viscosity (μ) is temperature-dependent and drops rapidly with increasing T.[37] The following viscosity−temperature equation is employed to describe this relationship

$$\mu(T) = \mu_0\, e^{-b(T-T_0)} \tag{12}$$

where the $\mu(T)$ is the viscosity at the temperature T, μ_0 is the viscosity at the reference temperature T_0, and b is the viscosity−temperature coefficient.

Because the droplet film is extremely thin, the change of viscosity in the height direction, z, can be ignored, whereas in the radial direction, the viscosity is changed with increasing of R_A and R_B and it can be considered as a function of the position r

$$\mu(x) = \mu_0\, e^{-b[(T_S - C_T r) - T_0]} \tag{13}$$

where T_S is the temperature at the starting position.

As mentioned above, the theoretical derivation is based on the assumption that the migration at each time interval is quasi-steady. To make the prediction more accurate, instead of substituting the viscosity−temperature equation into the integration formula (eq 7) directly, the viscosity at the middle position of outside and inside diameters of the ring, that is, at the position of $r = (R_A + R_B)/2$, is employed in the calculation. Using the force balance $F_v = F_d$ and combining eqs 7, 11, and 13, the migration velocity U can be derived as

$$U = \frac{\gamma_T C_T[4\cos\theta(R_B - R_A) + (R_B + R_A)]}{12\mu_T(R_B + R_A)}\frac{Q}{A} \tag{14}$$

where $\mu_T = \mu_0\, e^{-b[T_S - C_T(\frac{R_A+R_A}{2}) - T_0]}$, Q (constant value, 5 μL in this study) is the volume of the droplet, and A is the apparent area of the annulus liquid.

As described in the Experimental Section, the area A and the position of R_A and R_B during the migration process are measured. Because the contact angle of paraffin oils on the solid surface is very small (<10°), the difference of contact angles between the preceding and descending sides could be ignored and the value of cos θ is assumed to be 1.

3. EXPERIMENTAL SECTION

Figure 3 shows the experimental apparatus designed for this investigation. All migration experiments were performed on the circular substrate made of SUS 316 stainless steel with dimensions of 76 mm in diameter and 3 mm in thickness. The substrate is attached to a heating rod and a cooling ring equipped with a water cooling system to maintain its temperature at the desired values. In this fashion, an omnidirectional thermal gradient can be generated on the surface. The omnidirectional thermal gradient is confirmed by the thermography, and its value is measured by the thermocouples. As the thermography shown in Figure 3, the thermal gradient is nearly in a linear fashion in the radial direction, and the measured data of temperature are extracted from the center to the corners of the

DOI: 10.1021/acs.langmuir.7b04259
Langmuir 2018, 34, 3806−3812

thermography. When regarding the thermal gradient as a constant value, the slope standard error is about 2.95%, and a part of the error is from the system error of the temperature measurement equipment. Therefore, to simplify the process of analysis and calculation, we adapted the thermal gradient as a constant value. The migration procedure involves placing a precise volume of the paraffin oil droplets at the center and capturing the migration process with a digital camera. Via the extracted key frames, the droplet height h and the position r of inner and outer edges were obtained.

Paraffin oil (n-C_nH_{2n+2}) is a mixture of n-paraffin hydrocarbon with no additives, and the value of n is about 16−20. In this study, paraffin oils (Sinopec Yangzi Petrochemical Company, Nanjing, China) with two different kinematic viscosities were employed in this study. The dosage of the droplet was kept as a constant value of 5 μL, and the main physical parameters of paraffin oils are listed in Table 1.[30]

Table 1. Physical Parameters of Paraffin Oils at 40 °C

parameter	symbol	paraffin oil-1	paraffin oil-2
kinematic viscosity, mm^2/s	υ	13.4	26.9
density, g/cm^3	P	0.82904	0.8322
surface tension coefficient, mN/(m °C)	γ_T	0.082	0.081
viscosity temperature coefficient	B	0.02414	0.02784

4. RESULTS AND DISCUSSION

4.1. Basic Migration Phenomenon. Figure 4 shows the migration results of paraffin oil droplets on a surface subjected to an omnidirectional thermal gradient of 3.0 °C/mm. Key frames of the detailed dynamic migration process (paraffin oil with a viscosity of 26.9 mm^2/s) for the initial 6 s are shown in Figure 4a. When a droplet is placed onto the surface, it retains the natural shape and under the effect of an omnidirectional thermal gradient, the droplet migrates uniformly from the center outward, forming a ring. As time elapses, the ringlike shape is maintained and the diameter of the annulus liquid increases gradually. Figure 4b shows that a similar experimental phenomenon is observed with a less viscous droplet of 13.6 mm^2/s; however, the diameter of the annulus liquid is larger than that of 26.9 mm^2/s as the migration progresses.

This interfacial phenomenon is very unique, and the question is why the droplet migrates in the form of a ring? Because the interfacial tension of liquids decreases with increasing temperature, the droplet travels from the low-tension to high-tension regions. When placing a droplet on a surface subjected to an omnidirectional thermal gradient, the solid−liquid interfacial tension at the periphery edge of the droplet is larger than that at the rear edge. Thus, an interfacial gradient is generated, propelling the droplet to migrate from the center outward. Moreover, the internal force, $F_{Internal}$, (shown in Figure 2) of the droplet acting on the adjoining liquid provides an equilibrium condition in the circumferential direction and contributes to the homogeneous omnidirectional movement. Consequently, the droplet migrates like a ring with growing radius.

Figure 5 shows the quantitative migration results for the droplet with a viscosity of 26.9 mm^2/s. The droplet position r

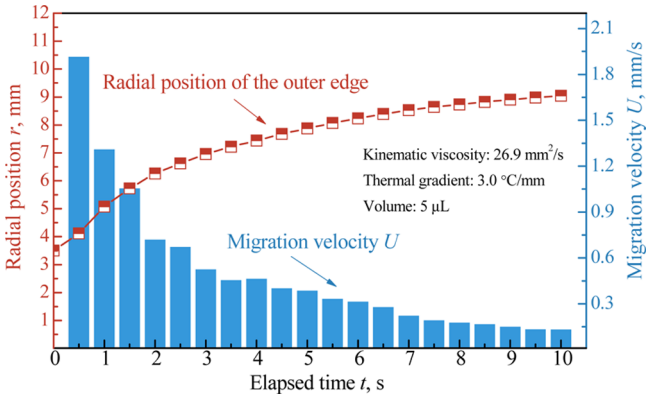

Figure 5. Droplet position r and migration velocity U vs elapsed time for a paraffin oil droplet with a viscosity of 26.9 mm^2/s.

and migration velocity U are measured at the outer edge of the droplet in the radial direction and plotted as a function of time. It can be seen from the line-symbol graph that the radial position increases quickly at first, and as time elapses, it increases slowly. Accordingly, as the histogram shows, the migration velocity is initially rapid, slows down gradually, and finally diminishes close to zero.

4.2. Validation of Model. The expression derived for the migration velocity U shows that it has a direct relationship with the apparent area A of the annulus liquid. Figure 6 shows the apparent area A of the liquid annulus obtained by analyzing the images of migration process via an image processing software. It

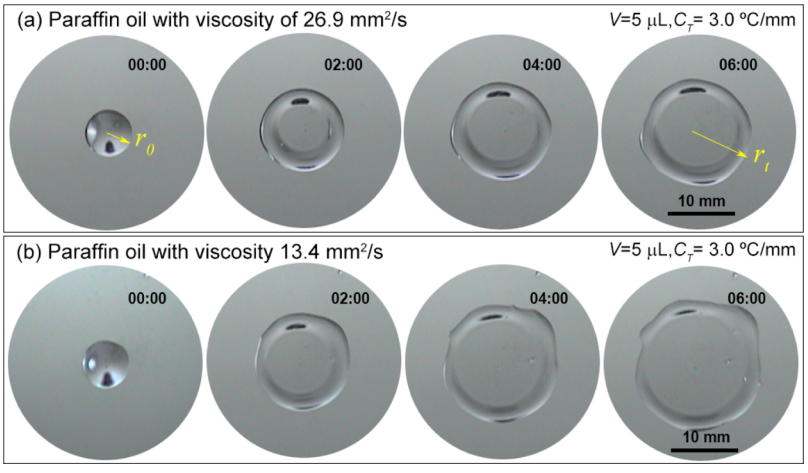

Figure 4. Migration results of paraffin oil droplets on a surface subjected to an omnidirectional thermal gradient: (a) viscosity of 26.9 mm^2/s and (b) viscosity of 13.6 mm^2/s.

DOI: 10.1021/acs.langmuir.7b04259
Langmuir 2018, 34, 3806−3812

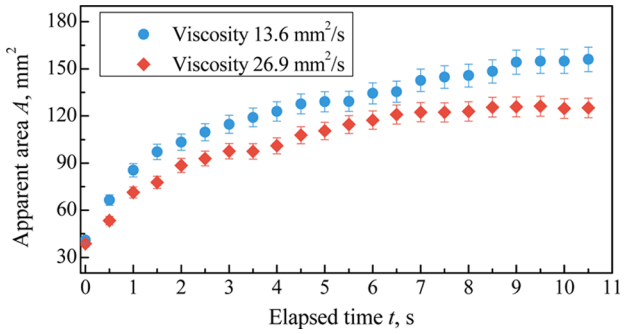

Figure 6. Apparent area A of the annulus liquid vs elapsed time for paraffin oil droplets with different viscosities.

can be seen that the apparent area for liquid droplets with different viscosities is nearly the same at first but increases gradually as time elapsed. As expected intuitively, the paraffin oil with a lower viscosity yields a larger apparent area. Having determined the apparent area, the theoretical migration velocity can be calculated.

Figure 7a shows a comparison between the experimental and theoretical velocity for the migration phenomenon presented in

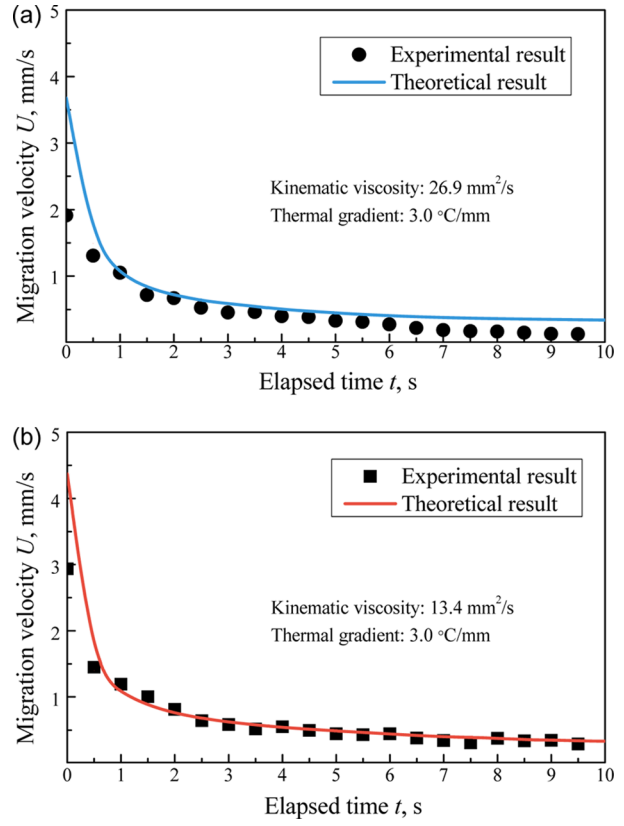

Figure 7. Comparison of the experimental and theoretical results for paraffin oil droplet migration under an omnidirectional thermal gradient of 3.0 °C/mm with different kinematic viscosities: (a) 26.9 and (b) 13.4 mm²/s.

Figure 4a. The average migration velocity at the outside edge (R_B) of the droplet is calculated and plotted as a function of time. As the diagram shows, the experimental migration velocity is approximate 1.9 mm/s initially, and it decreases rapidly in the first few seconds and becomes nil as time elapses. The line graph in Figure 7 shows that the theoretical results are consistent with the experimental data in both trend and magnitude, although a slight difference exists at the beginning.

To further verify the validity of the theoretical model, the experimental results with a paraffin oil droplet with a kinematic viscosity of 13.4 mm²/s (shown in Figure 4b) are also compared. As shown in Figure 7b, the beginning migration velocity is about 3.0 mm/s and it decreases as time elapses. Compared to Figure 7a, the migration velocity increases with decreasing initial viscosity. This changing trend is predicted by eq 14, and the comparison of experimental results shows that the predicted velocities are in good agreement in both trend and magnitude.

4.3. Further Discussion and Outlook. In the present model, we established an appropriate force balance at the outer and inner edges of the liquid annulus by developing a 2-D model wherein the unbalanced Young's force and viscous resistance constitute the propulsion force and the internal force contributes to the balance in the circumference. Because the droplet film is significantly thin, the ringlike migration is assumed to be a quasi-steady process. The theoretical results shown in Figure 7 are in accordance with the experimental data in both trend and magnitude. Nevertheless, slight differences exist at the beginning of the migration process because of the factors described next.

First, the velocity rapidly increases to its highest value and slows down gradually in the initial stage of the migration procedure; within that period of time, the shape of the droplet changes from that of a drop to an annulus. This initial acceleration is not included in our analysis because the theoretical model is set up after the ring is formed. Second, it is assumed that the droplet reaches the surface temperature as soon as it hits the surface. This starting temperature can play an important role in the initial acceleration phase, affecting the migration velocity. Third, although for the annulus liquid, the width far outweigh the height, regarding the height profile as a constant value can bring the errors. Moreover, neglecting the liquid remaining in the middle region may also cause some errors. These simplifications are the main reasons why the difference exists at the beginning of the migration process.

It is believed that a comprehensive consideration of the initial stage will be necessary to obtain more accurate predictions, at the expense of additional complications in the model and derivations. Moreover, with the introducing of the advanced particle image velocimetry technology, one could have an insight into this initial process and explain the mechanism. In general, most natural solid surfaces are rough and chemically heterogeneous; thus, the pinning of the contact line on defects of surfaces, wetting and dewetting processes for a liquid droplet on a solid surface will be affected.[38] Further, roughness investigation will make this theoretical derivation a lot more interesting and practical.

5. CONCLUSIONS

An experimentally verified model is developed to gain insight into the motion of the migration of a droplet subjected to omnidirectional thermal gradients. It is revealed that the unbalanced interfacial tension acting on the liquid in the radial direction provides the propulsion for the migration, whereas the internal force acting on the adjoining liquid contributes to the equilibrium condition in the circumferential direction. These are the primary cause of the ringlike migration, and the circumferential symmetry makes the theoretical derivation relatively easy to realize. By integrating the theoretical

DOI: 10.1021/acs.langmuir.7b04259
Langmuir 2018, 34, 3806−3812

expression of the migration velocity in the polar angle direction ($d\phi$), we arrived at an effective approach for estimating the theoretical velocity. This knowledge is important in applications where liquid lubricants are encountered with directionally unstable thermal gradients. Using this procedure, one can predict the migration rate of liquid lubricants for the design of lubrication systems. It can also be employed to induce a thermal gradient to drive liquid lubricants to reach and wet the rubbing surfaces as needed.

■ ASSOCIATED CONTENT

Supporting Information

The Supporting Information is available free of charge on the ACS Publications website at DOI: 10.1021/acs.langmuir.7b04259.

Ring migration process for a paraffin oil droplet with a viscosity of 26.9 mm^2/s (AVI)

Ring migration process for a paraffin oil droplet with a viscosity of 13.4 mm^2/s (AVI)

■ AUTHOR INFORMATION

Corresponding Author

*E-mail: wxl@nuaa.edu.cn. Phone/Fax: +86-25-84893630.

ORCID

Xiaolei Wang: 0000-0001-7422-4259

Notes

The authors declare no competing financial interest.

■ ACKNOWLEDGMENTS

The authors are grateful for the financial support provided by the National Natural Science Foundation of China (no. 51675268), the Fundamental Research Funds for the Central Universities (no. NE2017104), and the NUAA Research Funding (no. 1005-YAH17045).

■ REFERENCES

(1) Davis, S. H. Thermocapillary instabilities. *Annu. Rev. Fluid Mech.* **1987**, *19*, 403−435.

(2) Khonsari, M. M. A review of thermal effects in hydrodynamic bearings part i: Slider and thrust bearings. *ASLE Trans.* **1987**, *30*, 26−33.

(3) Smith, M. K. Thermocapillary migration of a two-dimensional liquid droplet on a solid surface. *J. Fluid Mech.* **1995**, *294*, 209−230.

(4) Daniel, S.; Chaudhury, M. K.; Chen, J. C. Fast drop movements resulting from the phase change on a gradient surface. *Science* **2001**, *291*, 633−636.

(5) Tadmor, R. Marangoni flow revisited. *J. Colloid Interface Sci.* **2009**, *332*, 451−454.

(6) Dai, Q.; Huang, W.; Wang, X. Surface roughness and orientation effects on the thermo-capillary migration of a droplet of paraffin oil. *Exp. Therm. Fluid Sci.* **2014**, *57*, 200−206.

(7) Tadmor, R. Drops that pull themselves up. *Surf. Sci.* **2014**, *628*, 17−20.

(8) Dai, Q.; Huang, W.; Wang, X. A surface texture design to obstruct the liquid migration induced by omnidirectional thermal gradients. *Langmuir* **2015**, *31*, 10154−10160.

(9) Chaudhury, M. K.; Chakrabarti, A.; Daniel, S. Generation of motion of drops with interfacial contact. *Langmuir* **2015**, *31*, 9266−9281.

(10) Bormashenko, E.; Bormashenko, Y.; Grynyov, R.; Aharoni, H.; Whyman, G.; Binks, B. P. Self-propulsion of liquid marbles: Leidenfrost-like levitation driven by marangoni flow. *J. Phys. Chem. C* **2015**, *119*, 9910−9915.

(11) Musin, A.; Grynyov, R.; Frenkel, M.; Bormashenko, E. Self-propulsion of a metallic superoleophobic micro-boat. *J. Colloid Interface Sci.* **2016**, *479*, 182−188.

(12) Wasan, D. T.; Nikolov, A. D.; Brenner, H. Droplets speeding on surfaces. *Science* **2001**, *291*, 605−606.

(13) Xu, X.; Luo, J. Marangoni flow in an evaporating water droplet. *Appl. Phys. Lett.* **2007**, *91*, 124102.

(14) Karapetsas, G.; Chamakos, N. T.; Papathanasiou, A. G. Thermocapillary droplet actuation: Effect of solid structure and wettability. *Langmuir* **2017**, *33*, 10838−10850.

(15) Tadmor, R. Approaches in wetting phenomena. *Soft Matter* **2011**, *7*, 1577−1580.

(16) Xu, W.; Xu, J.; Li, X.; Tian, Y.; Choi, C.-H.; Yang, E.-H. Lateral actuation of an organic droplet on conjugated polymer electrodes via imbalanced interfacial tensions. *Soft Matter* **2016**, *12*, 6902−6909.

(17) Karapetsas, G.; Matar, O. K.; Valluri, P.; Sefiane, K. Convective rolls and hydrothermal waves in evaporating sessile drops. *Langmuir* **2012**, *28*, 11433−11439.

(18) Balasubramaniam, R.; Subramanian, R. S. The migration of a drop in a uniform temperature gradient at large marangoni numbers. *Phys. Fluids* **2000**, *12*, 733.

(19) Yakhshi-Tafti, E.; Cho, H. J.; Kumar, R. Droplet actuation on a liquid layer due to thermocapillary motion: Shape effect. *Appl. Phys. Lett.* **2010**, *96*, 264101.

(20) Karapetsas, G.; Sahu, K. C.; Sefiane, K.; Matar, O. K. Thermocapillary-driven motion of a sessile drop: Effect of non-monotonic dependence of surface tension on temperature. *Langmuir* **2014**, *30*, 4310−4321.

(21) Chaudhury, K.; Chakraborty, S. Spreading of a droplet over a nonisothermal substrate: Multiple scaling regimes. *Langmuir* **2015**, *31*, 4169−4175.

(22) Fath, A.; Bothe, D. Direct numerical simulations of thermocapillary migration of a droplet attached to a solid wall. *Int. J. Multiphase Flow* **2015**, *77*, 209−221.

(23) Bjelobrk, N.; Girard, H.-L.; Subramanyam, S. B.; Kwon, H.-M.; Quéré, D.; Varanasi, K. K. Thermocapillary motion on lubricant-impregnated surfaces. *Phys. Rev. Fluids* **2016**, *1*, 063902.

(24) Singer, J. P. Thermocapillary approaches to the deliberate patterning of polymers. *J. Polym. Sci., Part B: Polym. Phys.* **2017**, *55*, 1649−1668.

(25) Tadmor, R.; Das, R.; Gulec, S.; Liu, J.; N'guessan, H. E.; Shah, M.; Wasnik, P. S.; Yadav, S. B. Solid−liquid work of adhesion. *Langmuir* **2017**, *33*, 3594−3600.

(26) Karapetsas, G.; Sahu, K. C.; Matar, O. K. Effect of contact line dynamics on the thermocapillary motion of a droplet on an inclined plate. *Langmuir* **2013**, *29*, 8892−8906.

(27) Dai, Q.; Khonsari, M. M.; Shen, C.; Huang, W.; Wang, X. On the migration of a droplet on an incline. *J. Colloid Interface Sci.* **2017**, *494*, 8−14.

(28) Brochard, F. Motions of droplets on solid surfaces induced by chemical or thermal gradients. *Langmuir* **1989**, *5*, 432−438.

(29) Ford, M. L.; Nadim, A. Thermocapillary migration of an attached drop on a solid surface. *Phys. Fluids* **1994**, *6*, 3183−3185.

(30) Dai, Q.; Khonsari, M. M.; Shen, C.; Huang, W.; Wang, X. Thermocapillary migration of liquid droplets induced by a unidirectional thermal gradient. *Langmuir* **2016**, *32*, 7485−7492.

(31) Moumen, N.; Subramanian, R. S.; McLaughlin, J. B. Experiments on the motion of drops on a horizontal solid surface due to a wettability gradient. *Langmuir* **2006**, *22*, 2682−2690.

(32) Subramanian, R. S.; Moumen, N.; McLaughlin, J. B. Motion of a drop on a solid surface due to a wettability gradient. *Langmuir* **2005**, *21*, 11844−11849.

(33) Daniel, S.; Chaudhury, M. K. Rectified motion of liquid drops on gradient surfaces induced by vibration. *Langmuir* **2002**, *18*, 3404−3407.

(34) Mettu, S.; Chaudhury, M. K. Motion of drops on a surface induced by thermal gradient and vibration. *Langmuir* **2008**, *24*, 10833−10837.

DOI: 10.1021/acs.langmuir.7b04259
Langmuir 2018, 34, 3806−3812

(35) Pratap, V.; Moumen, N.; Subramanian, R. S. Thermocapillary motion of a liquid drop on a horizontal solid surface. *Langmuir* **2008**, *24*, 5185−5193.
(36) De Gennes, P. G. Wetting: Statics and dynamics. *Rev. Mod. Phys.* **1985**, *57*, 827−863.
(37) Seeton, C. J. Viscosity−temperature correlation for liquids. *Tribol. Lett.* **2006**, *22*, 67−78.
(38) Bormashenko, E. Progress in understanding wetting transitions on rough surfaces. *Adv. Colloid Interface Sci.* **2015**, *222*, 92−103.

DOI: 10.1021/acs.langmuir.7b04259
Langmuir 2018, 34, 3806−3812